

## Article

## Biochemical and Mechanistic Characterization of the fungal reverse *N*-1-Dimethylallyltryptophan Synthase DMATS1

Immo Burkhardt, Zhongfeng Ye, Slavica Janevska, Bettina Tudzynski, and Jeroen S. Dickschat

*ACS Chem. Biol.*, **Just Accepted Manuscript** • DOI: 10.1021/acscchembio.9b00828 • Publication Date (Web): 22 Nov 2019

Downloaded from [pubs.acs.org](https://pubs.acs.org) on November 28, 2019

### Just Accepted

“Just Accepted” manuscripts have been peer-reviewed and accepted for publication. They are posted online prior to technical editing, formatting for publication and author proofing. The American Chemical Society provides “Just Accepted” as a service to the research community to expedite the dissemination of scientific material as soon as possible after acceptance. “Just Accepted” manuscripts appear in full in PDF format accompanied by an HTML abstract. “Just Accepted” manuscripts have been fully peer reviewed, but should not be considered the official version of record. They are citable by the Digital Object Identifier (DOI®). “Just Accepted” is an optional service offered to authors. Therefore, the “Just Accepted” Web site may not include all articles that will be published in the journal. After a manuscript is technically edited and formatted, it will be removed from the “Just Accepted” Web site and published as an ASAP article. Note that technical editing may introduce minor changes to the manuscript text and/or graphics which could affect content, and all legal disclaimers and ethical guidelines that apply to the journal pertain. ACS cannot be held responsible for errors or consequences arising from the use of information contained in these “Just Accepted” manuscripts.

# Biochemical and Mechanistic Characterization of the fungal reverse *N*-1-Dimethylallyltryptophan Synthase DMATS1<sub>Ff</sub>

Immo Burkhardt,<sup>#,‡</sup> Zhongfeng Ye,<sup>#,‡</sup> Slavica Janevska,<sup>§</sup> Bettina Tudzynski,<sup>§</sup> and Jeroen S. Dickschat<sup>#,\*</sup>

<sup>#</sup> Kekulé Institut für Organische Chemie und Biochemie, Rheinische Friedrich Wilhelms-Universität Bonn, Gerhard-Domagk-Str. 1, 53121 Bonn, Germany

<sup>§</sup> Institut für Biologie und Biotechnologie der Pflanzen, Westfälische Wilhelms-Universität Münster, Schlossplatz 8, 48143 Münster, Germany.

**ABSTRACT:** Dimethylallyltryptophan synthases catalyze the regiospecific transfer of (oligo)-prenylpyrophosphates to aromatic substrates like tryptophan derivatives. These reactions are key steps in many biosynthetic pathways of fungal and bacterial secondary metabolites. *In vitro* investigations on recombinant DMATS1<sub>Ff</sub> from *Fusarium fujikuroi* identified the enzyme as the first selective reverse tryptophan-*N*-1 prenyltransferase of fungal origin. The enzyme was also able to catalyze the reverse *N*-geranylation of tryptophan. DMATS1<sub>Ff</sub> was shown to be phylogenetically related to fungal tyrosine *O*-prenyltransferases and fungal 7-DMATS. Like these enzymes, DMATS1<sub>Ff</sub> was able to convert tyrosine into its regularly *O*-prenylated derivative. Investigation of the binding sites of DMATS1<sub>Ff</sub> by homology modeling and comparison to the crystal structure of 4-DMATS FgaPT2 showed an almost identical site for DMAPP binding, but different residues for tryptophan coordination. Several putative active site residues were verified by site directed mutagenesis of DMATS1<sub>Ff</sub>. Homology models of the phylogenetically related enzymes showed similar tryptophan binding residues, pointing to a unified substrate binding orientation of tryptophan and DMAPP, which is distinct from that in FgaPT2. Isotopic labeling experiments showed the reaction catalyzed by DMATS1<sub>Ff</sub> to be non-stereospecific. Based on these data, a detailed mechanism for DMATS1<sub>Ff</sub> catalysis is proposed.

Prenylations are ubiquitous biochemical modifications that significantly influence the overall polarity of biomolecules and thus their activity and availability within a living cell. Examples are post-translational prenylations of proteins<sup>1</sup> and peptides<sup>2</sup> as well as prenylation steps in the biosynthesis of important primary metabolites like ubiquinones.<sup>3</sup> Prenylations also occur in biosyntheses of microbial secondary metabolites, where they produce intermediates that allow for structural diversification towards a plethora of bioactive alkaloids or non-ribosomal peptides.<sup>4,5</sup> These reactions are usually carried out by prenyltransferases belonging to the ABBA superfamily.<sup>6</sup> The common overall fold of this superfamily consists of five repeating  $\alpha\beta\alpha$  structural elements, which result in a barrel of 10 antiparallel  $\beta$ -sheets that harbors the active site.<sup>7,8</sup> These enzymes catalyze the regioselective prenylation of aromatic substrates in a Friedel-Crafts alkylation.<sup>9</sup> Many of them utilize tryptophan (Trp, **1**) or tryptophan derivatives and dimethylallyl pyrophosphate (DMAPP, **2**) as substrates and thus make up the group of dimethylallyltryptophan synthases (DMATS).<sup>10</sup> Enzymes for the regioselective prenylation with DMAPP are known for every available (non-bridgehead) position of the electron rich aromatic indole nucleus (Figure 1).<sup>11</sup> Further, prenylation of the indole ring can proceed by nucleophilic attack at C-1 or C-3 of DMAPP, resulting in “regular” or “reverse” prenylation (Figure 1).<sup>10</sup> Regularly prenylated **3** is the first intermediate in the biosynthesis of ergot alkaloids in *Aspergillus* spp. and *Claviceps* spp.,<sup>12</sup> while reversely *N*-1-prenylated **4** is known as a building block for the NRPS derived antibiotics ilamycin from *Streptomyces atratus*<sup>13</sup> and the cyclomarins from *Salinispora arenicola*.<sup>14</sup> Although most DMATS members are known from filamentous fungi, **4** is a building block only occurring in bacterial natural products.<sup>11</sup>

The general reaction mechanism of DMATS is thought to follow an S<sub>N</sub>1 reaction with generation of an isoprenyl cation and subsequent attack of the nucleophile, but although several DMATS are characterized to date, the mechanistic details including the origin of regio- and stereoselectivity as well as substrate selectivity of the particular enzymes is still not completely understood.<sup>10,15,16</sup>

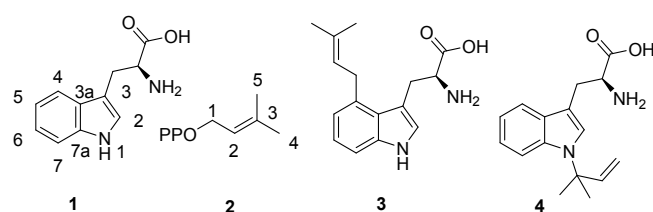


**Figure 1.** Carbon numbering of the indole nucleus in tryptophan (**1**) and of DMAPP (**2**). The structures **3** and **4** are examples for regular C-4- and reverse *N*-1-prenylations.

Despite the fact that no alkaloids or non-ribosomal peptides that contain prenylated tryptophan are known from *Fusarium* spp., five putative DMATS-coding genes were identified in genome sequenced members of the *Fusarium fujikuroi* species complex.<sup>17,18</sup> Two of the putative enzymes, DMATS1 and DMATS3, are coded on the genome of the rice pathogen *F. fujikuroi* IMI58289.<sup>18</sup> Genomic analysis showed DMATS1 to be part of a putative gene cluster, but only the *in vivo* overexpression of *dmats1* itself showed an impact on the metabolome, i.e. the occurrence of **4** and derivatives in extracts from mutant cultures.<sup>19</sup> Although the natural function of DMATS1 stayed unclear, these data suggested that it catalyzes reverse *N*-1-prenylation on **1**. Since this modification on free tryptophan was unknown from fungal biochemistry before, we

now report on the *in vitro* characterization of DMATS1 from *F. fujikuroi* (from now on called DMATS1<sub>Ff</sub>), including the biochemical characterization, substrate scope screening, as well as mechanistic investigations based on structural data from homology modeling, site directed mutagenesis and isotopic labeling experiments.

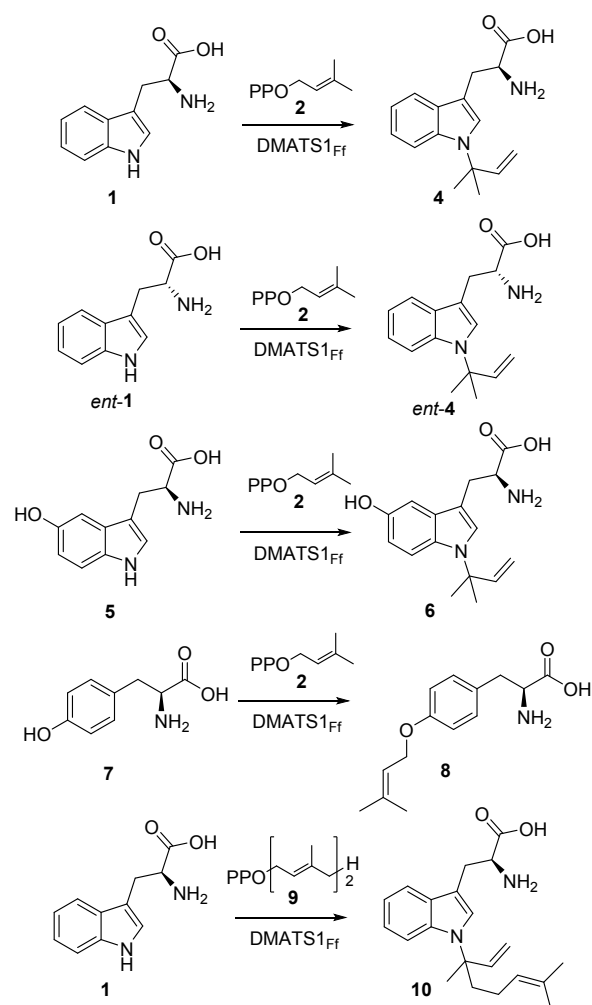
## RESULTS AND DISCUSSION

**Cloning, heterologous expression and *in vitro* activity of DMATS1<sub>Ff</sub>.** The gene coding for DMATS1<sub>Ff</sub> was obtained from the gDNA of *F. fujikuroi* IMI58289<sup>19</sup> and cloned into the expression vector pYE-express.<sup>20</sup> The expression construct was transformed into *Escherichia coli* BL21 (DE3). Standard expression conditions and purification *via* Ni-NTA affinity-chromatography yielded soluble hexahis-DMATS1<sub>Ff</sub> (Figure S1). *In vitro* incubations with L-tryptophan and DMAPP in Tris-buffer at pH 7.5 at room temperature yielded one new compound. A large-scale incubation, product purification by RP18-column chromatography and NMR-analysis confirmed that DMATS1<sub>Ff</sub> selectively catalyzes the production of **4** (Table S1) that was identified by comparison of NMR-spectroscopic data to those of a synthetic standard (Figure S2).<sup>21,22</sup>

**Biochemical characterization and substrate scope.** The optimum *in vitro* parameters were examined by comparison of the substrate conversion within 5 min reaction time. The temperature optimum was found at 35 °C (Figure S3). The pH values were tested in a range from 6 to 9 and showed no clear maximum, as the enzyme reached similar conversion rates at pH values between 7.0 and 9.0 (Figure S4). DMATS1<sub>Ff</sub> showed no dependency on divalent metal cations, but addition of Mg<sup>2+</sup> and Ca<sup>2+</sup> led to slightly enhanced reaction rates. This behavior was also reported for other DMATS.<sup>12,23,24</sup> Addition of different transition-metal cations inhibited the reactivity (Figure S5). Since studies on other DMATS showed substrate promiscuity,<sup>25,26,27</sup> the substrate scope of DMATS1<sub>Ff</sub> was surveyed by testing different tryptophan derivatives and structurally related compounds (Figure S6). For substrates missing either the free amino group or the free carboxylic acid group no product formation was observed. Histidin and *N*-1-methyl tryptophan as alternative amino acids were also not converted. Selective conversion was shown for the alternative substrates D-tryptophan (*ent*-1), 5-hydroxy-L-tryptophan (**5**) and L-tyrosine (**7**) (Figures S7-10). The observed conversion of *ent*-1 was low and the product was identified by HPLC comparison to **4**, showing the same retention time on a non-chiral column (Figures S7 and S8). For substrates **5** and **7** a better conversion was observed and large scale incubations were conducted. The products were purified by RP18-column chromatography and their structures were determined by one and two-dimensional NMR analysis as **6** and **8**, respectively (Tables S2 and S3). While tryptophan derived substrates were reversely prenylated at the *N*-1 position of the indole system, tyrosine (**7**) was selectively converted into the regularly *O*-prenylated compound **8**.

The prenyl donor DMAPP (**2**) was alternated to its isomer isopentenyl pyrophosphate (IPP) and the higher homologs geranyl pyrophosphate (GPP, **9**), farnesyl pyrophosphate (FPP) and geranylgeranyl pyrophosphate (GGPP) (Figure S11). While IPP, FPP and GGPP did not show conversion, faint product formation was observed when DMATS1<sub>Ff</sub> was incubated with **9** as a cosubstrate (Figure S12). A large scale incubation experiment with **1** and **9** was conducted and the product was purified by RP18-column chromatography and HPLC. The

structure of the product was unambiguously elucidated by 1- and 2-dimensional NMR spectroscopy as the novel compound **10**, showing an unusual reverse *N*-geranylation of the indole substructure (Scheme 1, Table S4). The geranylation of tryptophan was only reported for two 6-DMATS from *Streptomyces violaceusniger* and *Streptomyces ambofaciens* that both produced 6-geranyl tryptophan.<sup>28</sup> Fungal DMATS usually do not accept GPP instead of DMAPP, but lately enzyme variants of the 4-DMATS FgaPT2<sup>29</sup> and several diketopiperazine (DKP) converting DMATS<sup>30</sup> obtained by site directed mutagenesis were shown to produce geranylated products. The only occurrence of reverse *N*-geranylation on the indole nucleus was reported as one of four products from the incubation of a F335G mutant of CdpC3PT with cyclo-Trp-Val.<sup>30</sup> Thus, the selective enzymatic reverse *N*-geranylation on an indole moiety as catalyzed by DMATS1<sub>Ff</sub> is unprecedented.



**Scheme 1.** *In vitro* reactions of DMATS1<sub>Ff</sub> with different substrates.

The kinetic parameters of DMATS1<sub>Ff</sub> for the different identified substrates were determined to quantify the substrate selectivity (Table 1, Figure S13). Tryptophan (**1**) showed a  $k_{cat}$  value of 1.27 s<sup>-1</sup> and a  $K_m$  value of 0.31 mM. The alternative prenyl acceptor **5** was also converted well and showed a higher  $k_{cat}$  value than **1**, probably due to its higher electron density in the indole system, which promotes a faster nucleophilic attack. The  $K_m$  value, however, was approximately 18 times higher than for **1**, showing a much lower affinity towards DMATS1<sub>Ff</sub>. The catalytic efficiency ( $k_{cat}/K_m$ ) of tyrosine (**7**) conversion was 400

times smaller than that of **1**, and *ent-1* was converted even slower, the catalytic efficiency dropping by four orders of magnitude compared to the reaction with **1**. In a kinetic comparison of DMAPP (**2**) and GPP (**9**), DMAPP shows a more than 800 times higher  $k_{\text{cat}}$  value. The small apparent  $K_m$  value of 5  $\mu\text{M}$  observed in the conversion of **9** is accompanied by strong substrate inhibition with a  $K_i$  value of 278  $\mu\text{M}$  (Figures S13F). At a concentration of 2 mM, the product formation was already too slow to be measurable. These data show a clear preference of **1** as the prenyl acceptor and of **2** as the prenyl donor by DMATS<sub>1Fr</sub> among the tested substrates.

**Comparison of DMATS<sub>1Fr</sub> with other characterized DMATS.** A phylogenetic comparison of characterized DMATS-type prenyltransferases, which convert tyrosine (**5**), tryptophan (**1**) or tryptophan-containing diketopiperazines (DKPs), showed a clear separation of fungal and bacterial enzymes (Figure 2). Consequently, the two characterized bacterial DMATS CymD and IlaO that are responsible for reverse *N*-prenylation of **1** in the biosynthesis of cyclomarin and ilamycin do not show the highest sequence similarity to DMATS<sub>1Fr</sub>. Instead, the two characterized fungal tyrosine *O*-prenyltransferases SirD from *Leptosphaeria maculans*<sup>31</sup> and TyrPT from *Aspergillus niger*<sup>32</sup> form a branch with DMATS<sub>1Fr</sub>. These enzymes are also able to use **1** as a substrate to produce regularly 7-prenylated tryptophan (**11**).<sup>31,32</sup> SirD also produces small amounts of **4** as a second product, when incubated *in vitro* with **1**.<sup>33</sup> The biochemically characterized 7-DMATS from *Aspergillus fumigatus* and its homolog from *Aspergillus fischeri* are located next to the branch that contains DMATS<sub>1Fr</sub> and take tryptophan as the preferred substrate to produce **11**, but

are also able to convert tyrosine to **8**.<sup>34</sup> Thus, the named enzymes are related regarding their sequences and their substrate and product scopes (Scheme 2A). All the product structures can be explained by the same relative orientation of the substrates to each other (Scheme 2B), which suggests a common substrate binding mode for the named DMATS. The other two tryptophan converting fungal enzymes FgaPT2 and 5-DMATS<sub>Ac</sub> that show distinct regioselectivity are closer related to the DKP converting DMATS (Figure 2).

**Table 1.** Kinetic data for the conversion of different substrates by DMATS<sub>1Fr</sub>.

substrate	$k_{\text{cat}}$ [ $\text{s}^{-1}$ ] <sup>a</sup>	$K_m$ [mM] <sup>a</sup>	$k_{\text{cat}}/K_m$ [ $\text{s}^{-1} \cdot \text{mM}^{-1}$ ] <sup>a</sup>
<b>1</b> <sup>b</sup>	1.27±0.08	0.31±0.02	4.07±0.40
<b>5</b> <sup>b</sup>	2.26±0.13	5.61±0.54	0.40±0.05
<b>7</b> <sup>b</sup>	$(5.6 \pm 1.0) \cdot 10^{-3}$	3.40±1.88	$(1.0 \pm 0.6) \cdot 10^{-2}$
<i>ent-1</i> <sup>b</sup>	$(3.8 \pm 1.1) \cdot 10^{-3}$	7.94±3.35	$(4.8 \pm 2.4) \cdot 10^{-4}$
<b>2</b> <sup>c</sup>	0.69±0.04	0.34±0.08	1.99±0.45
<b>9</b> <sup>c,d</sup>	$(8.4 \pm 1.1) \cdot 10^{-4}$	0.005±0.002	0.16±0.07

*a*: values and standard errors determined from the fit of the Michaelis Menten equation to the data. *b*: determined with 2 mM of **2**. *c*: determined with 1 mM of **1**. *d*: **9** showed strong substrate inhibition above concentrations of 0.005 mM ( $K_i = 0.28 \pm 0.10$  mM).

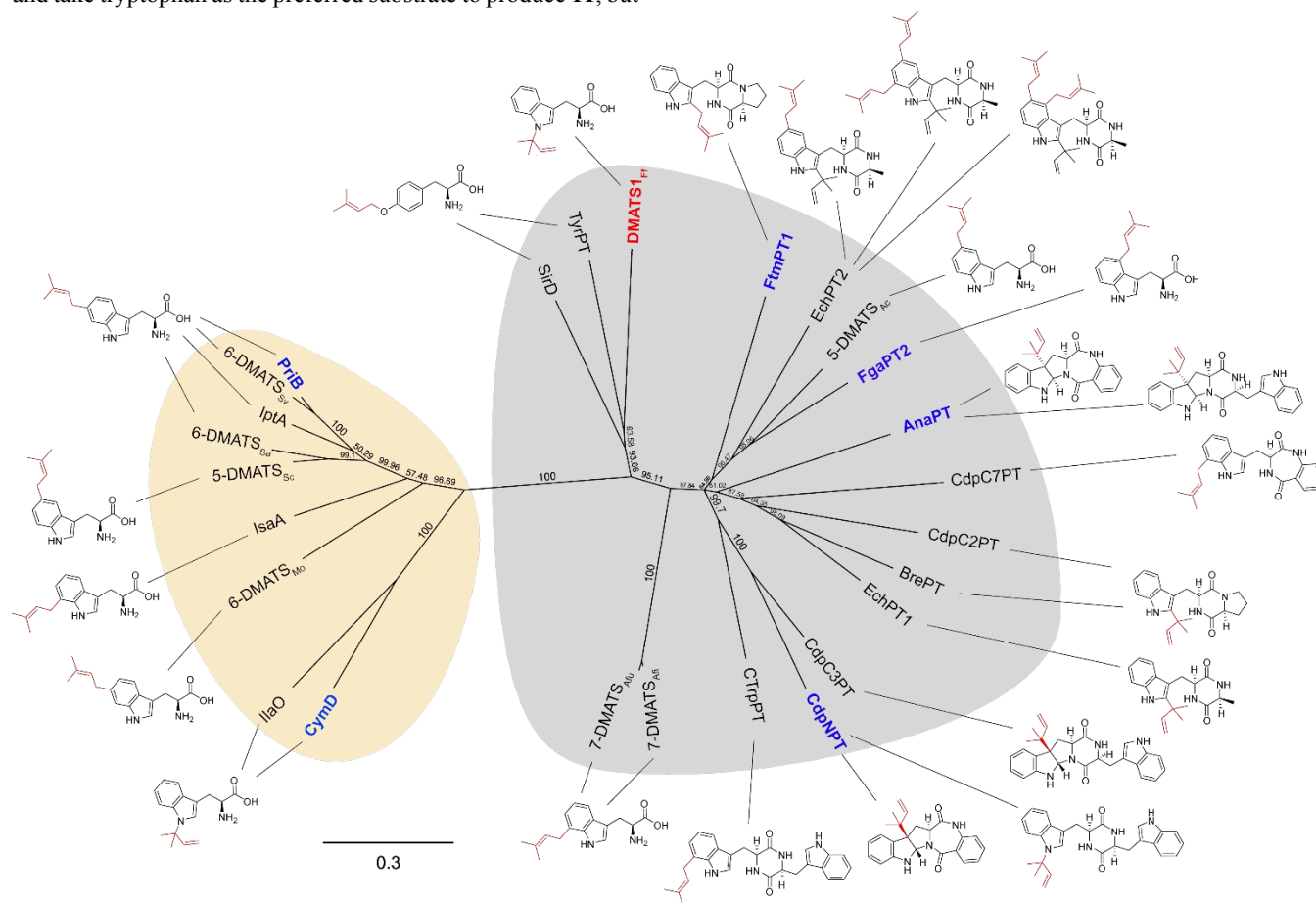
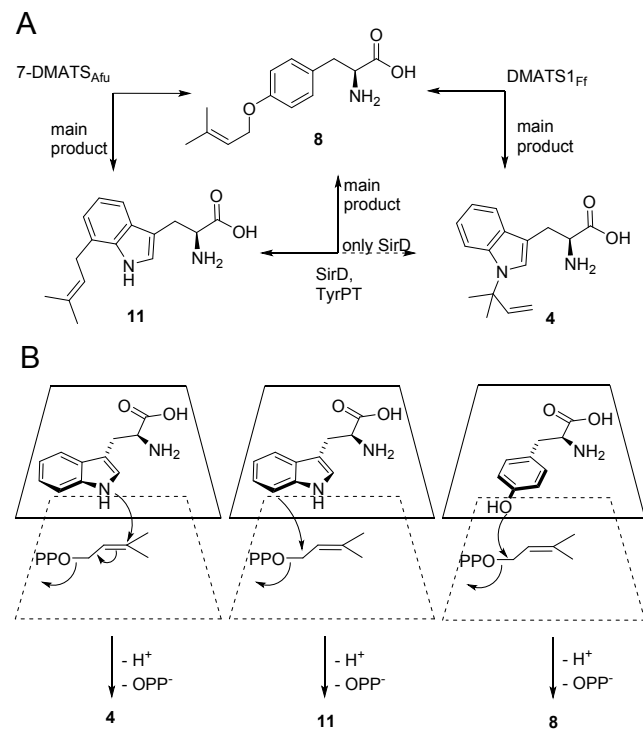


**Figure 2.** Phylogenetic tree of characterized DMATS. Bacterial and fungal enzymes form two clades as indicated by yellow and gray background. DMATS<sub>1FF</sub> is marked in red, names of enzymes with available crystal structures are marked in blue. The scale shows changes per site, numbers at branches are bootstrap values. For accession numbers and further information see Table S5.



**Scheme 2.** A: Products of phylogenetically related DMATS when incubated with either tyrosine or tryptophan. B: The same relative orientation of the two respective substrates facilitate regular *C*-7- and reverse *N*-1-prenylation of tryptophan as well as the *O*-prenylation of tyrosine.

**Active site analysis and mutagenesis of DMATS<sub>1FF</sub>.** To gain insights into the orientation of the substrates, a homology model of DMATS<sub>1FF</sub> was generated using the SWISS model server and the ligand-bound crystal structure of FgaPT2<sup>8</sup> (PDB code: 3I4X) as the template (Figure S14). The homology model of DMATS<sub>1FF</sub> showed the same conserved active site residues compared to the structures of FgaPT2 (Figure S15) or the DKP prenyltransferase FtmPT1.<sup>35</sup> Docking of the substrates tryptophan (**1**) and DMAPP (**2**) into the active site of the model in a similar manner as observed in the FgaPT2 crystal structure explain the formation of **4** (Figure 3). The pyrophosphate group of DMAPP is surrounded by two rings of polar residues (Figures 3A and 3B). The first ring consists of K187, K253, K332 and R105, the second ring is composed of Y189, Y255, Y334 and Y404. Despite K332 all these residues are highly conserved in the enzymes included in Figure 2 (Figure S16).<sup>36</sup> To check the importance of these residues for catalysis in DMATS<sub>1FF</sub>, a library of enzyme variants was constructed and their kinetics were measured (Table 2, Figures S17 and S18). Exchanges of K187, K253 and R105 against Met, and of Y189, Y255 and Y404 against Phe resulted in a clearly diminished catalytic efficiency ( $k_{cat}/K_m$ ) in comparison to the wild type in all cases (Table 2). R251 is located near the active site and part of the highly conserved **RXKXY** motif that is found in all DMATS discussed in this work (Figure S16). This residue was exchanged by Met and Lys. While the R251M variant showed 21% catalytic efficiency of the wild type enzyme, the R251K variant retained 58%. R105 is in close proximity to **2** in its

bound state, and the R105K variant exhibited only 9% of the catalytic efficiency of the wild type. These data hint towards distinct roles of the two conserved Arg residues. While R105 probably tightly interacts with the pyrophosphate group of **2** during catalysis, R251 could be more important for substrate and product transport, which can also be promoted by the charged Lys side chain.

Besides these conserved residues, K332 and S400 are unique to DMATS<sub>1FF</sub> and are both placed in proximity to the pyrophosphate. The corresponding positions are occupied by Q343 and Y409 in FgaPT2 (Figure S15). The K332Q and S400Y variants showed 50% and 56% catalytic efficiency, and **4** was observed as the only product in both cases, suggesting a non-critical role for both residues.

The putative binding site for **1** was also investigated (Figures 3C and 3D). The indole system of **1** is oriented in parallel to the prenyl unit of **2** and closes the hydrophobic cavity (Figure 3B). Since the prenyl acceptors are more variable between different DMATS, not many conserved residues are found in this part of the active site. One exception is a conserved E90 in DMATS<sub>1FF</sub> (Figure 3C), which is capable of forming a hydrogen bond with the indole nitrogen *N*-1 (Figure S15).<sup>36</sup> Its exchange against Ala (E90A) led to a completely inactive enzyme, as has been demonstrated for FgaPT2.<sup>8</sup> Also as in FgaPT2, two unpolar amino acids (F81 and M82 in DMATS<sub>1FF</sub>) point their amide oxygens inside the active site, providing hydrogen bondings to the  $\alpha$ -amino group of **1** (Figures 3 and S15). Via the adjacent S80 these two residues are connected to a hydrogen bonding network, the central point of which is the highly conserved E109 in DMATS<sub>1FF</sub> (Figure S16 and S19). The E109M variant showed drastically reduced catalytic efficiency of less than 1% of the wild type. Especially the  $K_m$  for **1** was strongly elevated, pointing to an important role of binding of **1**.

Differences in the tryptophan binding site of FgaPT2 compared to DMATS<sub>1FF</sub> are exhibited by the three polar residues K174, Y191 and R244 that are positioned near **1** in the FgaPT2 active site (Figure S15B and C). In FgaPT2, K174 is possibly involved in the final deprotonation towards the product **3** at indole position *C*-4,<sup>37</sup> while Y191 and R244 interact with **1** via hydrogen bonds to the carboxylic acid function.<sup>8</sup> In the model structure of DMATS<sub>1FF</sub> the corresponding three positions are occupied by F174, I191 and F238, which are all not suitable for polar interactions with **1**. However, Arg257 is located near F238 on the neighboring beta sheet and could interact with the carboxylic acid moiety of **1** through hydrogen bonds (Figure 3C). While it was not possible to heterologously express recombinant DMATS<sub>1FF</sub>-F174K, the variants I191Y, F238R and R257L all showed below 2% residual catalytic efficiency of the wild type (Table 2), with significantly higher  $K_m$  values. The strongest effect was observed for the R257L variant, by a near 15-fold increase of the  $K_m$ . These data suggest that all three amino acid exchanges disfavor the binding of **1**. Since R257 is the only positively charged residue in the tryptophan binding site of DMATS<sub>1FF</sub>, it is probably responsible for interacting with the tryptophan carboxylic acid moiety by formation of a salt bridge and thus enables correct substrate orientation (Figure 3C and D). Elimination of this polar charge or introduction of other polar groups could lead to wrong binding, lowering the enzymatic affinity towards **1** and thus hamper catalysis.

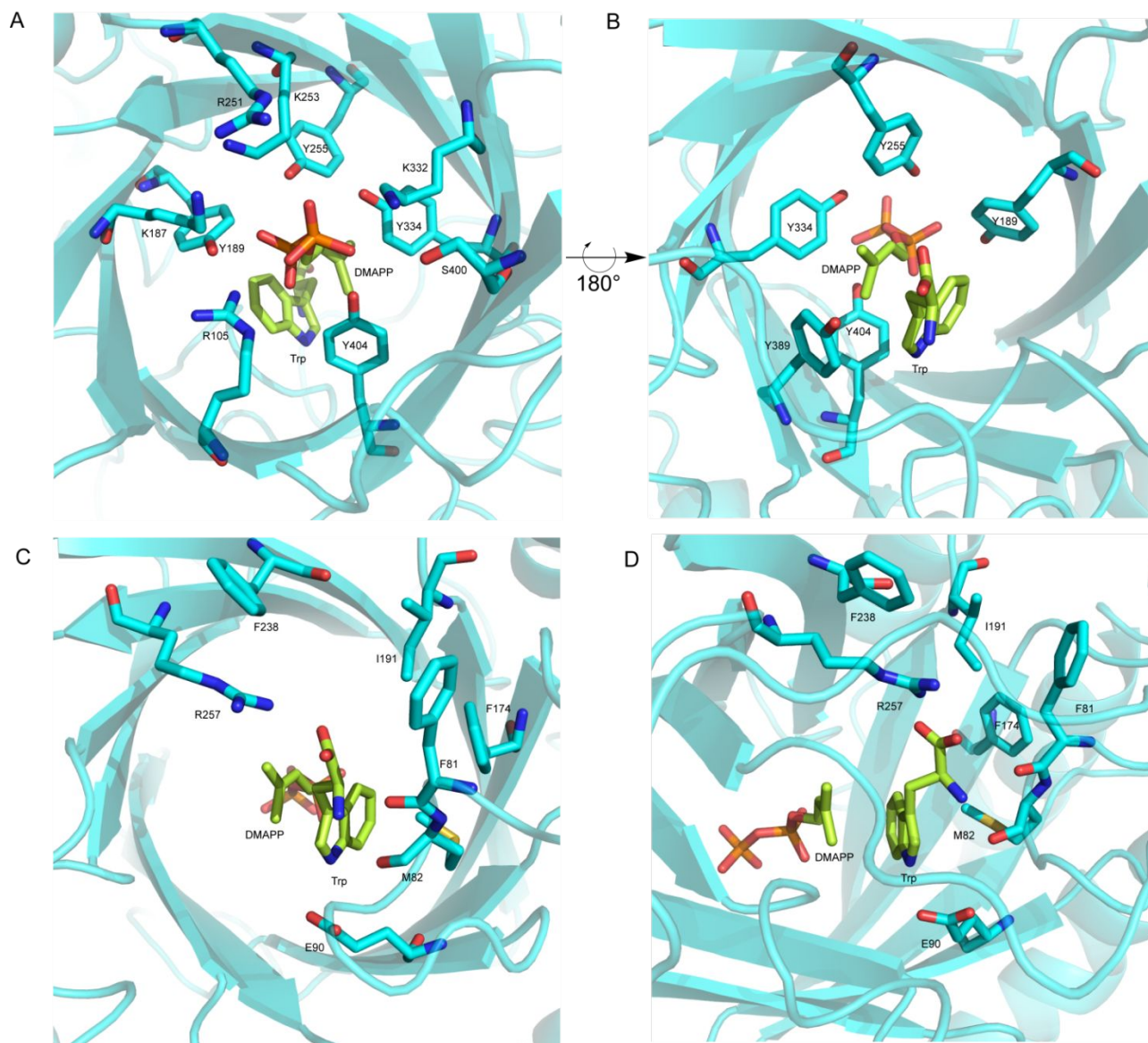


**Figure 3.** Graphic representation of the DMATS1<sub>Ff</sub> homology model (blue) with docked substrates (green). **A** and **B**: Binding site for 2. **C** and **D**: Binding site for 1.

**Table 2. Kinetic data for the conversion of 1 and 2 by different variants of DMATS1<sub>Ff</sub>.**

DMATS1 <sub>Ff</sub> variant	$k_{\text{cat}}$ (s <sup>-1</sup> ) <sup>a</sup>	$K_{\text{m}}$ (mM) <sup>a</sup>	$k_{\text{cat}}/K_{\text{m}}$ [s <sup>-1</sup> *mM <sup>-1</sup> ] <sup>a</sup>	DMATS1 <sub>Ff</sub> variant	$k_{\text{cat}}$ (s <sup>-1</sup> ) <sup>a</sup>	$K_{\text{m}}$ (mM) <sup>a</sup>	$k_{\text{cat}}/K_{\text{m}}$ [s <sup>-1</sup> *mM <sup>-1</sup> ] <sup>a</sup>
E90A	n. m. <sup>b</sup>	n. m. <sup>b</sup>	n. m. <sup>b</sup>	R251K	2.87±0.15	1.20±0.17	2.40±0.37
R105K	0.10±0.01	0.27±0.11	0.38±0.16	R251M	0.12±0.01	0.13±0.05	0.87±0.31
R105M	0.16±0.02	0.66±0.25	0.24±0.09	K253M	0.02±0.00	0.38±0.22	0.06±0.03
E109M	0.16±0.03	7.89±2.32	0.02 ±0.01	Y255F	0.06±0.00	0.06±0.01	0.98±0.22
K187M	0.21±0.01	0.22±0.05	0.98±0.22	R257L	0.44±0.03	4.53±0.59	0.10±0.02
I191Y	0.10±0.01	1.14±0.34	0.09±0.03	K332Q	0.72±0.02	0.36±0.05	2.02±0.27
Y189F	0.03±0.00	0.11±0.04	0.24±0.09	S400Y	1.49±0.08	0.66±0.11	2.27±0.39
F238R	0.11±0.01	2.10±0.23	0.05±0.01	Y404F	n. m. <sup>b</sup>	n. m. <sup>b</sup>	n. m. <sup>b</sup>

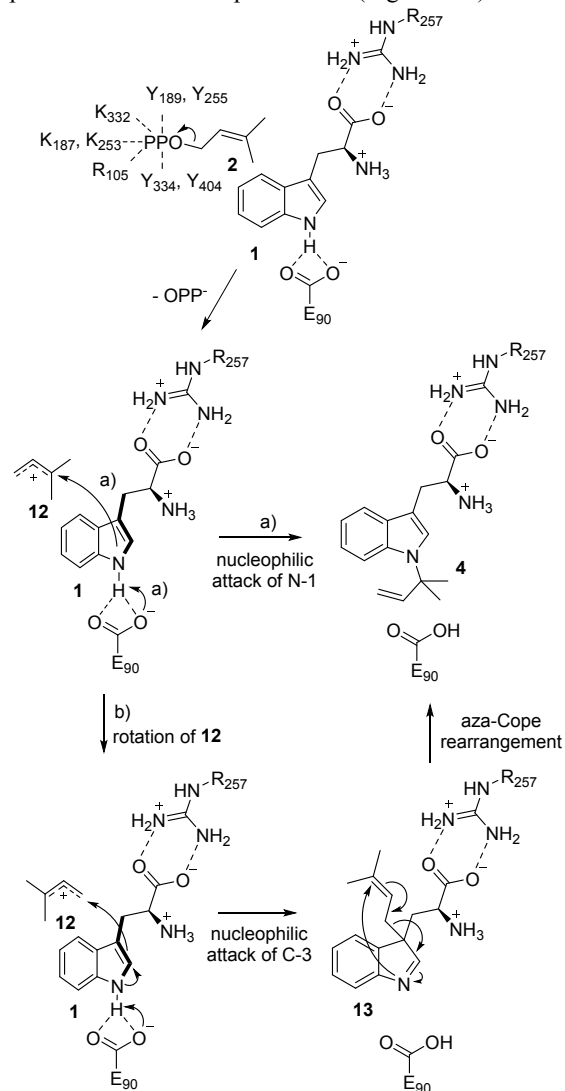
<sup>a</sup>: values and standard errors determined from the fit of the Michaelis Menten equation to the data. <sup>b</sup>: n. m. = not measurable.

Since the exchange of non-conserved R257 resulted in a severely diminished catalytic efficiency, the other fungal DMATS were compared regarding the occurrence of an Arg in the putative amino acid binding site. Such a residue could indeed be observed for 7-DMATS<sub>Afi</sub>, 7-DMATS<sub>Afi</sub>, TyrPT and SirD two positions downstream the **RXKXY** motif (Figure S16). Structural models were created, showing that the corresponding Arg residues for DMATS1<sub>Ff</sub>, 7-DMATS<sub>Afi</sub>, TyrPT and SirD are all located at the same position (Figure S20). In contrast, none of the DKP-DMATS models exhibited a corresponding Arg in the prenyl-acceptor binding site. Thus, an Arg residue seems to be vital for amino acid-prenyltransferases, while the uncharged, larger DKPs cannot interact with such a residue, which is consequently not needed for catalysis. This is further supported by mutagenesis studies on FgaPT2, in which the enzyme showed better catalytic parameters towards DKPs,<sup>38,39</sup> and worse towards **1**,<sup>40</sup> after R244 was substituted.

Also tyrosine (**7**) was docked into the model structure of DMATS1<sub>Ff</sub> (Figure S21). Tyrosine (**7**) can adopt a similar orientation as **1**, which would allow for the coordination of the acid group to R257, and of the amino group towards F91 and M92, while the aromatic ring lies in parallel to **2** and closes the hydrophobic pocket. This binding mode is in line with the proposed relative substrate orientations shown in Scheme 2 and places the phenolic oxygen of **7** in closer proximity to C-1 rather than C-3 of DMAPP (**2**), in contrast to the findings for substrate **1**. E90 is not positioned accordingly to interact with the phenolic hydroxyl group in the docked structure but may be flexible enough to reach a fitting orientation (Scheme S1). In this manner, the reverse *N*-prenylation of **1** and the regular *O*-prenylation of **7** by DMATS<sub>Ff</sub> can be explained.

**The reaction mechanism of DMATS1<sub>Ff</sub>.** By combining the results of the model structure analysis of the binding site, the site directed mutagenesis experiments and the characterized products, a detailed reaction mechanism of DMATS1<sub>Ff</sub> can be proposed (Scheme 3). Since the DMAPP binding site is highly conserved among DMATS, the pyrophosphate abstraction from **2** is likely the same as in all related enzymes. Thus, the polar residues around the bound pyrophosphate facilitate its abstraction by tight coordination to produce the allyl cation **12** is shielded by the hydrophobic cavity, which is closed by the aromatic substrate (Figure 3B). Tryptophan (**1**) is held in the right position by the polar interactions of R257 and the amide carbonyl groups of F81 and M82, while E90 coordinates to the amine hydrogen of the indole ring, thereby increasing the nucleophilicity of *N*-1 (Figures 3C and 3D). The relative positioning of the substrates **1** and **2** suggests a direct attack by the indole nitrogen at C-3 of **2** in which E90 could serve as the base to deprotonate *N*-1 in a concerted reaction (Scheme 3, path a). For the bacterial enzyme CymD, which also selectively produces **4**, a reaction mechanism involving a nucleophilic attack of the indole C-3 position at C-1 of DMAPP (**2**) and a subsequent aza-Cope rearrangement was discussed (path b), since the nitrogen of the aromatic indole system is a rather weak nucleophile.<sup>42</sup> However, our homology-based structural model is in favor of a direct inverse *N*-1 prenylation. A rotation of cation **12** of more than 90° would be necessary to enable the reaction of path b, which makes this mechanism less likely than the direct attack by the indole nitrogen.

A recently published crystal structure of substrate bound CymD strongly suggests a direct nucleophilic attack also in that case.<sup>43</sup> Despite the similar reaction mechanisms, the active site architectures of CymD and DMATS1<sub>Ff</sub> disclose strong differences. While for DMATS1<sub>Ff</sub> binding of the substrates results in a similar aromatic cavity as in FgaPT2 (Figure S15), DMAPP and tryptophan are found with inverted relative orientation in the CymD crystal structure.<sup>43</sup> Further, CymD does not seem to coordinate significantly to the polar residues of the amino acid side chain. This is indicated on the one hand by the substrate positioning in the substrate bound crystal and on the other hand by the distinct substrate scope, as indole was converted equally fast as **1** and turnover of *ent*-**1** was only four times slower,<sup>43</sup> which is in contrast to the findings for DMATS1<sub>Ff</sub> from this work. A mechanism, analogous to the reverse prenylation of **1** can also be assumed for the regular prenylation of **7** in DMATS1<sub>Ff</sub> (Scheme S1). The role of E90 is not clear in this case, but it may be flexible enough to reach the phenol OH of **7** for deprotonation (Figure S21).



**Scheme 3.** Proposed reaction mechanism of DMATS1<sub>Ff</sub> by direct reverse *N*-1 prenylation (path a) and alternative mechanism by normal *C*-3 prenylation and aza-Cope rearrangement (path b).

**Stereochemical course of the prenylation.** The stereoselectivity of the reaction was surveyed by isotopic labelling experiments. Regioselectively labeled (4-<sup>13</sup>C)IPP

(14)<sup>44</sup> was transformed *in situ* into (4-<sup>13</sup>C)-2 using the isopentenyl diphosphate isomerase from *Serratia plymuthica* (IDI<sub>Sp</sub>)<sup>45</sup> and directly converted by DMATS1<sub>Ff</sub> in a one-pot reaction with **1** as a cosubstrate (Figure 4A). Since the methyl groups of **4** are diastereotopic, they show two distinct signals in the <sup>13</sup>C-NMR spectrum of **4** (Figure 4B). The resulting spectrum from the labeling experiment showed strongly enhanced signal intensities for both methyl groups in **4** with a ratio of 4:1 (Figure 4C and S22). To exclude an impact of IDI<sub>Sp</sub> on this outcome, a control reaction was carried out, using the enzyme in a coupled assay with FPP synthase from *Streptomyces coelicolor*<sup>46</sup> and isodaucenol synthase from *Streptomyces venezuelae*<sup>47</sup> for the production of stereoselectively <sup>13</sup>C-labeled isodaucenol, proving complete stereoselectivity of IDI<sub>Sp</sub> (Figure S23).

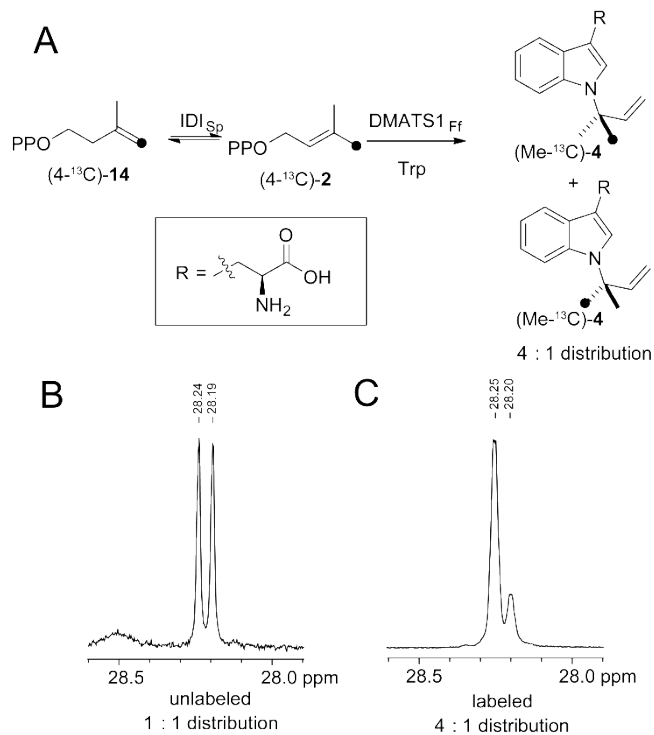


**Figure 4.** A: Enzymatic conversion of (4-<sup>13</sup>C)-**14** into labeled **4**. B: <sup>13</sup>C-NMR signals for the methyl groups of unlabeled **4**. C: <sup>13</sup>C-NMR signals for the methyl groups of labeled **4** obtained from (4-<sup>13</sup>C)-**14**.

These findings imply that the observed isotopic scrambling occurs during catalysis by DMATS1<sub>Ff</sub>. The distribution of the methyl labeling must be caused by switching of *Re* and *Si* attack from **1** to **2** and thus by a change of the relative substrate orientations. This could originate from rotation of the prenyl cation **12** before the reaction with **1**, or from different initial substrate binding modes. To distinguish between these two scenarios, the stereochemical course of the dephosphorylation was analyzed. Since the sp<sup>3</sup> center at C-1 in DMAPP (**2**) is converted to a planar sp<sup>2</sup> center during formation of cation **12** and is preserved in the final product, the prochiral CH<sub>2</sub> hydrogen atoms at this position are converted into *E*- and *Z*-oriented hydrogens, which are distinguishable in <sup>1</sup>H,<sup>13</sup>C-HSQC spectroscopy (Figures 5B and 5C). To track the hydrogen atoms through the reaction, a new set of incubation experiments was carried out using (*R*)- and (*S*)-(1-<sup>2</sup>H,1-<sup>13</sup>C)-**2**,<sup>48</sup> which were converted *in situ* into (*R*)- and (*S*)-(1-<sup>2</sup>H,1-<sup>13</sup>C)-**2** by IDI<sub>Sp</sub> and then directly by DMATS1<sub>Ff</sub> into labeled **4** (Figure 5A). The resulting simultaneously <sup>13</sup>C- and <sup>2</sup>H-labeled positions are suitable for sensitive analysis by HSQC spectroscopy, in which

the signals for the <sup>2</sup>H-labeled hydrogen positions do not appear. In this experiment a scrambling of the isotopic labeling was observed, again with a distribution of 4:1, leading to mainly *Z*-labeled **4** from (*R*)-(1-<sup>2</sup>H,1-<sup>13</sup>C)-**14** (Figure 5D) and mainly *E*-labeled **4** from (*S*)-(1-<sup>2</sup>H,1-<sup>13</sup>C)-**14** (Figure 5E). Since the distribution of labeling from the geminal methyl groups and the enantiotopic C-1 hydrogens of DMAPP occurs with the same ratio, it is unlikely that a rotation of the prenyl cation in the active site is responsible for the isotopic scrambling of the methyl groups, because this would not influence the fate of the C-1 hydrogen atoms in **4**. Also, a bond rotation between C-1 and C-2 after formation of cation **12** is unlikely, because of the high rotational barrier in allyl cations.<sup>49</sup> Instead, different substrate binding modes for **2** in the active site of DMATS1<sub>Ff</sub> provide a more likely explanation (Scheme 4). The main isotopomers observed in both <sup>2</sup>H-labeling experiments can be explained by the substrate orientations as shown in Figure 3, with the pyrophosphate leaving to the *Re* face at C-1 of DMAPP, in conjunction with the indole-nitrogen attacking at the *Re* face of C-3 (Scheme 4A). In this way, the 1-*pro-R* hydrogen of **2** becomes H<sub>Z</sub> in **4** and the 1-*pro-S* hydrogen becomes H<sub>E</sub>. A second binding mode of **2** is sterically similarly demanding but exhibits a stereochemically distinct orientation in the active site (Scheme 4B).

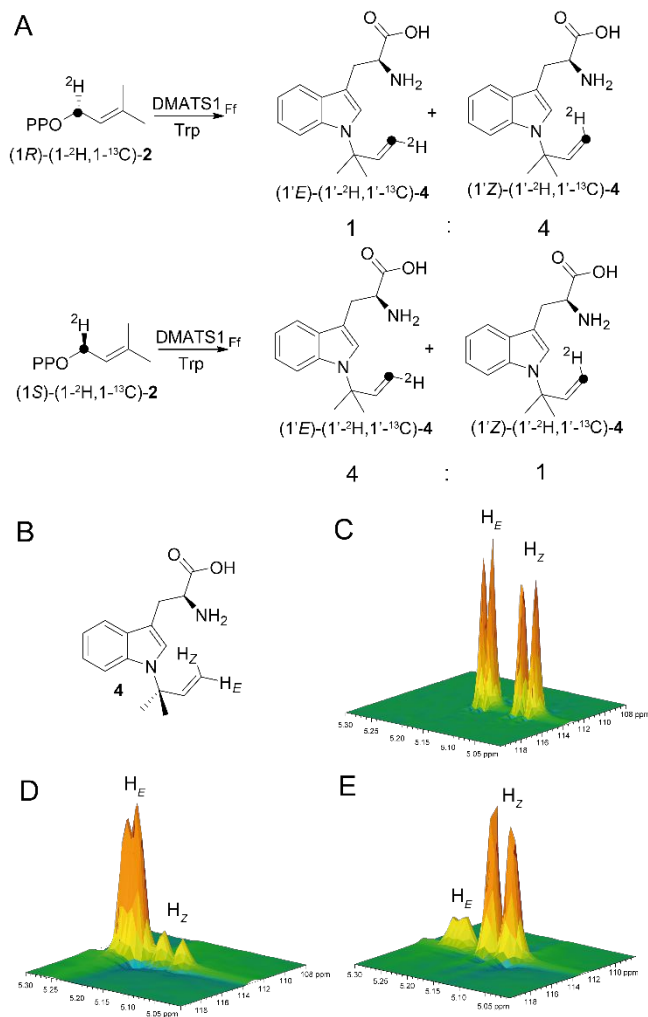
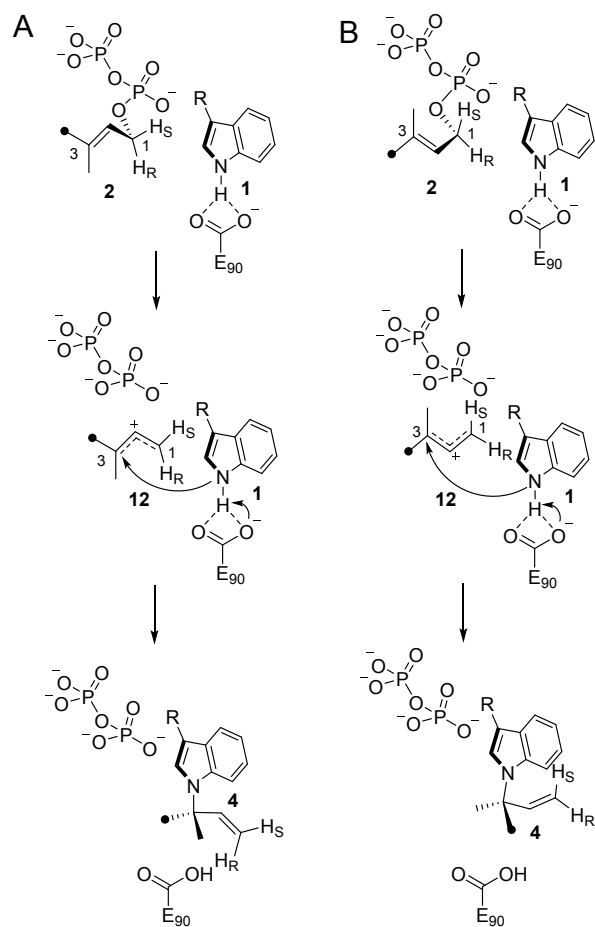


**Figure 5.** A: Incubation experiments with *in situ* generated (*R*)-(1-<sup>2</sup>H,1-<sup>13</sup>C)-**2** (up) and (*S*)-(1-<sup>2</sup>H,1-<sup>13</sup>C)-**2** (down). B: Indicated positions of the observed H<sub>Z</sub> and H<sub>E</sub> atoms in **4**. C: HSQC-signals for H<sub>Z</sub> and H<sub>E</sub>. D: HSQC

signals resulting from the incubation with (*R*)-(1-<sup>2</sup>H,1-<sup>13</sup>C)-**2**. **E**: HSQC signals resulting from the incubation with (*S*)-(1-<sup>2</sup>H,1-<sup>13</sup>C)-**2**.



**Scheme 4.** Proposed stereochemical reaction pathways that explain the observations from the labeling experiments. **A**: Major reaction path. **B**: Minor reaction path.

Starting from this alternative relative substrate orientation, the pyrophosphate leaves to the *Si* face at C-1 of **12**, with attack of the indole nitrogen from the *Si* face of C-3. This reaction results in the opposite outcome for the C-1 hydrogens of **2**, i.e. the 1-*pro-R* hydrogen ends up in the *E* position and the 1-*pro-S* hydrogen in the *Z* position of the vinyl group in **4**.

## CONCLUSION

In summary, the first reverse prenylating *N*-1-dimethylallyltryptophan synthase from a fungus, DMATS<sub>1Ff</sub>, was characterized *in vitro*. The enzyme was shown to accept **1**, *ent*-**1**, and **5** as prenyl acceptors for selective reverse *N*-prenylation and **7** as prenyl acceptor for selective regular *O*-prenylation. DMATS<sub>1Ff</sub> was able to catalyze the unprecedented reverse *N*-geranylation of **1**. A homology model of DMATS<sub>1Ff</sub> in comparison to the crystal structure of FgaPT2 allowed for site directed mutagenesis of single active site residues in DMATS<sub>1Ff</sub>. The strongest effect was seen for the R257L variant by a rise of the  $K_m$ . This finding is in line with an interaction between R257 and the substrate **1** through a salt bridge. A corresponding arginine residue is observed in all enzymes that employ a putative similar binding mode for prenylation on the “downside” of **1**, while FgaPT2 and the closely related 5-DMATS<sub>Ac</sub> that prenylate on the “upside” of the indole moiety show different polar residues for the interaction with **1**,

including an Arg that is placed distinctively (Figure 6). DKP-converting DMATS do not show such an active site Arg, making this residue probably one of the factors responsible for substrate selection.

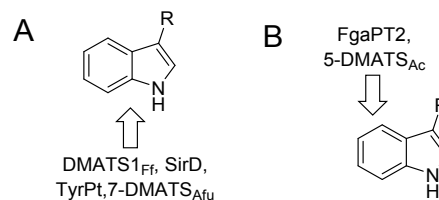


**Figure 6.** **A**: Enzymes catalyzing “downside” indole prenylation. **B**: Enzymes catalyzing “upside” prenylation.

The combined data shed light on the reaction mechanisms of DMATS<sub>1Ff</sub> and related amino acid prenyltransferases. In the case of DMATS<sub>1Ff</sub> a direct attack of the indole nitrogen at C-3 of **2** takes place, followed by deprotonation by E90 at the same nitrogen (Scheme 3) is the most likely scenario. A mechanism including an aza-Cope rearrangement on the other hand seems unlikely because of the relative orientations of the substrates, which would require a major rotation of the prenyl cation. The incubations with stereoselectively labeled **2** in this work showed clear scrambling of the labeled positions by the reaction of DMATS<sub>1Ff</sub>, which can be explained by relaxed binding modes of **2** in the active site, but not by a rotation of the prenyl cation **12**. The occurrence of more than one reaction course displays a certain dynamic freedom in the active site, subtle changes of which could be responsible for the distinct prenylation regiochemistry of different enzymes that start from the same substrate binding modes. This might be caused by different active site residues or by small changes in the overall three-dimensional structure of the enzymes and will have to be further investigated in future studies to gain a comprehensive understanding of how DMATS enzymes accomplish their remarkable regioselectivity.

## ASSOCIATED CONTENT

**Supporting Information.** Experimental procedures including general and analytical methods, cloning, site-directed mutagenesis, heterologous expression of proteins, *in vitro* incubation experiments, structural elucidation of enzymatic products, kinetic analyses, *in silico* analyses, NMR-spectra, supporting figures, schemes and tables. This material is available free of charge *via* the Internet at <http://pubs.acs.org>.

## AUTHOR INFORMATION

### Corresponding Author

\* Email: [dickschat@uni-bonn.de](mailto:dickschat@uni-bonn.de)

### Author Contributions

‡ These authors contributed equally to this work. I.B., Z.Y. and S.J. performed the experimental work. J.S.D. and B.T. designed the research. The manuscript was written by I.B. and J.S.D. with proofreading by all other authors.

### Funding Sources

This work was supported by the DFG with grant DI1536/9-1.

### Notes

The authors declare no competing financial interest.

## ACKNOWLEDGMENT

We thank A. J. Schneider for HPLC analyses and A. Babczyk for the synthesis of **4** and experimental assistance.

## REFERENCES

- (1) Palsuledesai, C. C. and DiStefano, M. D. (2015) Protein Prenylation: Enzymes, Therapeutics, and Biotechnology Applications. *ACS Chem. Biol.* *10*, 51-62.
- (2) Sugita, T., Okada, M., Nakashima, Y., Tian, T. and Abe I. (2018) A Tryptophan Prenyltransferase with Broad Substrate Tolerance from *Bacillus subtilis* subsp. *natto*. *ChemBioChem* *19*, 1396-1399.
- (3) Li, W. (2016) Bringing Bioactive Compounds into Membranes: The UbiA Superfamily of Intramembrane Aromatic Prenyltransferases. *Trends Biochem. Sci.* *41*, 357-370.
- (4) Li, S.-M. (2010) Prenylated indole derivatives from fungi: structure diversity, biological activities, biosynthesis and chemoenzymatic synthesis. *Nat. Prod. Rep.* *27*, 57-78.
- (5) Winkelblech, J. and Li, S.-M. (2015) Prenyltransferases as key enzymes in primary and secondary metabolism. *Appl. Microbiol. Biotechnol.* *99*, 7379-7397.
- (6) Tello, M., Kuzuyama, T., Heide, L., Noel, J. P. and Richard, S. B. (2008) The ABBA family of aromatic prenyltransferases: broadening natural product diversity. *Cell. Mol. Life Sci.* *65*, 1459-1463.
- (7) Kuzuyama, T., Noel, J. P. and Richard, S. B. (2005) Structural basis for the promiscuous biosynthetic prenylation of aromatic natural products. *Nature* *435*, 983-987.
- (8) Metzger, U., Schall, C., Zocher, G., Unsöld, I., Stec, E., Li, S.-M., Heide, L. and Stehle, T. (2009) The structure of dimethylallyl tryptophan synthase reveals a common architecture of aromatic prenyltransferases in fungi and bacteria. *Proc. Natl. Acad. Sci. USA* *106*, 14309-14314.
- (9) Gebler, J. C., Woodside, A. B. and Poulter, C. D. (1992) Dimethylallyltryptophan Synthase. An Enzyme-Catalyzed Electrophilic Aromatic Substitution. *J. Am. Chem. Soc.* *114*, 7354-7360.
- (10) Walsh, C. T. (2014) Biological Matching of Chemical Reactivity: Pairing Indole Nucleophilicity with Electrophilic Isoprenoids. *ACS Chem. Biol.* *9*, 2718-2728.
- (11) Fan, A., Winkelblech, J. and Li, S.-M. (2015) Impacts and perspectives of prenyltransferases of the DMATS superfamily for use in biotechnology. *Appl. Microbiol. Biotechnol.* *99*, 7399-7415.
- (12) Unsöld, I. A. and Li, S.-M. (2005) Overproduction, purification and characterization of FgaPT2, a dimethylallyltryptophan synthase from *Aspergillus fumigatus*. *Microbiology* *151*, 1499-1505.
- (13) Ma, J., Huang, H., Xie, Y., Liu, Z., Zhao, J., Zhang, C., Jia, Y., Zhang, Y., Zhang, H., Zhang, T. and Ju, J. (2017) Biosynthesis of ilamycins featuring unusual building blocks and engineered production of enhanced anti-tuberculosis agents. *Nat. Commun.* *8*, 391.
- (14) Schultz, A. W., Oh, D.-C., Carney, J. R., Williamson, R. T., Udvary, D. W., Jensen, P. R., Gould, S. J., Fenical, W. and Moore, B. S. (2008) Biosynthesis and Structures of Cyclomarins and Cyclomarazines, Prenylated Cyclic Peptides of Marine Actinobacterial Origin. *J. Am. Chem. Soc.* *130*, 4507-4516.
- (15) Tanner, M. E. (2015) Mechanistic studies on the indole prenyltransferases. *Nat. Prod. Rep.* *32*, 88-101.
- (16) Yu X., Zocher, G., Xie, X., Liebold, M., Schütz, S., Stehle, T. and Li, S.-M. (2013) Catalytic Mechanism of Stereospecific Formation of cis-Configured Prenylated Pyrroloindoline Diketopiperazines by Indole Prenyltransferases. *Chem. Biol.* *20*, 1492-1501.
- (17) Wiemann, P., Sieber, C. M. K., von Bargen, K. W., Studt, L., Niehaus, E.-M., Espino, J. J., Huß, K., Michielse, C. B., Albermann, S., Wagner, D., Bergner, S. V., Connolly, L. R., Fischer, A., Reuter, G., Kleigrew, K., Bald, T., Wingfield, B. D., Ophir, R., Freeman, S., Hippler, M., Smith, K. M., Brown, D. W., Proctor, R. H., Münsterkötter, M., Freitag, M., Humpf, H.-U., Güldener, U. and Tudzynski, B. (2013) Deciphering the Cryptic Genome: Genome-wide Analyses of the Rice Pathogen *Fusarium fujikuroi* Reveal Complex Regulation of Secondary Metabolism and Novel Metabolites. *PLOS Pathog.* *9*, e1003475.
- (18) Niehaus, E.-M., Münsterkötter, M., Proctor, R. H., Brown, D. W., Sharon, A., Idan, Y., Oren-Young, L., Sieber, C. M., Novák, O., Pencik, A., Tarkowská, D., Hromadová, K., Freeman, S., Maymon, M., Elazar, M., Youssef, S. A., El-Shabrawy, E. S. M., Shalaby, A. B. A., Houterman, P., Brock, N. L., Burkhardt, I., Tsavkelova, E. A., Dickschat, J. S., Galuszka, P., Güldener, U. and Tudzynski, B. (2016) Comparative "Omics" of the *Fusarium fujikuroi* Species Complex Highlights Differences in Genetic Potential and Metabolite Synthesis. *Genome Biol. Evol.* *8*, 3574-3599.
- (19) Arndt, B., Janevska, S., Schmid, R., Hübner, F., Tudzynski, B. and Humpf, H.-U. (2017) A Fungal *N*-Dimethylallyltryptophan Metabolite from *Fusarium fujikuroi*. *ChemBioChem.* *18*, 899-904.
- (20) Dickschat, J. S., Pahirulzaman, K. A. K., Rabe, P. and Klapschinski, T. A. (2014) An Improved Technique for the Rapid Chemical Characterisation of Bacterial Terpene Cyclases. *ChemBioChem.* *15*, 810-814.
- (21) Luzung, M. R., Lewis, C. A. and Baran, P. S. (2009) Direct, Chemoselective *N*-tert-Prenylation of Indoles by C-H Functionalization. *Angew. Chem. Int. Ed.* *48*, 7025-7029.
- (22) Schultz, A. W., Lewis, C. A., Luzung, M. R., Baran, P. S. and Moore, B. S. (2010) Functional Characterization of the Cyclomarlin/Cyclomarazine Prenyltransferase CymD Directs the Biosynthesis of Unnatural Cyclic Peptides. *J. Nat. Prod.* *73*, 373-377.
- (23) Gebler, J. C. and Poulter, C. D. (1992) Purification and Characterization of Dimethylallyl Tryptophan Synthase from *Claviceps pupurea*. *Arch. Biochem. Biophys.* *296*, 308-313.
- (24) Miyamoto, K., Ishikawa, F., Nakamura, S., Hayashi, Y., Nakanishi, I. and Kakeya, H. (2014) A 7-dimethylallyl tryptophan synthase from a fungal *Neosartorya* sp.: Biochemical characterization and structural insight into the regioselective prenylation. *Bioorg. Med. Chem.* *22*, 2517-2528.
- (25) Steffan, N., Unsöld, I. A. and Li, S.-M. (2007) Chemoenzymatic Synthesis of Prenylated Indole Derivatives by Using a 4-Dimethylallyltryptophan Synthase from *Aspergillus fumigatus*. *ChemBioChem.* *8*, 1298-1307.
- (26) Yu, X., Liu, Y., Xie, X., Zheng, X.-D. and Li, S.-M. (2012) Biochemical Characterization of Indole Prenyltransferases - Filling the last Gap of Prenylation Positions by a 5-Dimethylallyltryptophan Synthase from *Aspergillus clavatus*. *J. Biol. Chem.* *287*, 1371-1380.
- (27) Winkelblech, J., Xie, X. and Li, S.-M. (2016) Characterisation of 6-DMATS<sub>Mo</sub> from *Micromonospora olivasterospora* leading to identification of the divergence in enantioselectivity, regioselectivity and multiple prenylation of tryptophan prenyltransferases. *Org. Biomol. Chem.* *14*, 9883-9895.
- (28) Winkelblech, J. and Li, S.-M. (2014) Biochemical Investigations of Two 6-DMATS Enzymes from *Streptomyces* Reveal New Features of L-Tryptophan Prenyltransferases. *ChemBioChem.* *15*, 1030-1039.
- (29) Mai, P., Zocher, G., Stehle, T. and Li, S.-M. (2018) Structure-based protein engineering enables prenyl donor switching of a fungal aromatic prenyltransferase. *Org. Biomol. Chem.* *16*, 7461-7469.
- (30) Liao, G., Mai, P., Fan, J., Zocher, G., Stehle, T. and Li, S.-M. (2018) Complete Decoration of the Indolyl Residue in cyclo-L-Trp-L-Trp with Geranyl Moieties by Using Engineered Dimethylallyl Transferases. *Org. Lett.* *20*, 7201-7205.
- (31) Kremer, A. and Li, S.-M. (2010) A tyrosine *O*-prenyltransferase catalyzes the first pathway-specific step in the biosynthesis of sirodesmin PL. *Microbiology.* *156*, 278-286.
- (32) Fan, A., Chen, H., Wu, R., Xu, H. and Li, S.-M. (2014) A new member of the DMATS superfamily from *Aspergillus niger* catalyzes prenylations of both tyrosine and tryptophan derivatives. *Appl. Microbiol. Biotechnol.* *98*, 10119-10129.
- (33) Rudolf, J. D. and Poulter, C. D. (2013) Tyrosine *O*-Prenyltransferase SirD Catalyzes *S*<sup>-</sup>, *C*<sup>-</sup>, and *N*-Prenylations on Tyrosine and Tryptophan Derivatives. *ACS Chem. Biol.* *8*, 2707-2714.
- (34) Fan, A. and Li, S.-M. (2014) Prenylation of tyrosine and derivatives by a tryptophan C7-prenyltransferase. *Tetrahedron Lett.* *55*, 5199-5202.

- (35) Jost, M., Zocher, G., Tarcz, S., Matuschek, M., Xie, X., Li, S.-M. and Stehle, T. (2010) Structure-Function Analysis of an Enzymatic Prenyl Transfer Reaction Identifies a Reaction Chamber with Modifiable Specificity. *J. Am. Chem. Soc.* *132*, 17849-17858.
- (36) Liu, X. and Walsh, C. T. (2009) Characterization of cyclo-Acetoacetyl-L-Tryptophan Dimethylallyltransferase in Cyclopiiazonic Acid Biosynthesis: Substrate Promiscuity and Site Directed Mutagenesis Studies. *Biochemistry*. *48*, 11032-11044.
- (37) Luk, L. Y. P., Qian, Q. and Tanner, M. E. (2011) A Cope Rearrangement in the Reaction Catalyzed by Dimethylallyltryptophan Synthase? *J. Am. Chem. Soc.* *133*, 12342-12345.
- (38) Fan, A. and Li, S.-M. (2016) Saturation mutagenesis on Arg244 of the tryptophan C4-prenyltransferase FgaPT2 leads to enhanced catalytic ability and different preferences for tryptophan-containing cyclic dipeptides. *Appl. Microbiol. Biotechnol.* *100*, 5389-5399.
- (39) Zheng, L., Mai, P., Fan, A. and Li, S.-M. (2018) Switching a regular tryptophan C4-prenyltransferase to a reverse tryptophan containing cyclic dipeptide C3-prenyltransferase by sequential site-directed mutagenesis. *Org. Biomol. Chem.* *16*, 6688-6694.
- (40) Fan, A., Zocher, G., Stec, E., Stehle, T. and Li, S.-M. (2015) Site-directed Mutagenesis Switching a Dimethylallyl Tryptophan Synthase to a Specific Tyrosine C3-Prenylating Enzyme. *J. Biol. Chem.* *290*, 1364-1373.
- (41) Luk, L. Y. P. and Tanner, M. E. (2009) Mechanism of Dimethylallyltryptophan Synthase: Evidence for a Dimethylallyl Cation Intermediate in an Aromatic Prenyltransferase Reaction. *J. Am. Chem. Soc.* *131*, 13932-13933.
- (42) Qian, Q., Schultz, A. W., Moore, B. S. and Tanner, M. E. (2012) Mechanistic Studies on CymD: A Tryptophan Reverse N-Prenyltransferase. *Biochemistry* *51*, 7733-7739.
- (43) Roose, B. W. and Christianson, D. W. (2019) Structural Basis of Tryptophan Reverse N-Prenylation Catalyzed by CymD. *Biochemistry* *58*, 3232-3242.
- (44) Rabe, P., Rinkel, J., Dolja, E., Schmitz, T., Nubbemeyer, B., Luu, H. and Dickschat, J. S. (2017) Mechanistic Investigations of Two Bacterial Diterpene Cyclases: Spiroviolene Synthase and Tsukubadiene Synthase. *Angew. Chem. Int. Ed.* *56*, 2776-2779.
- (45) Rinkel, J., Lauterbach, L., Rabe, P. and Dickschat, J. S. (2018) Two Diterpene Synthases for Spiroalbatene and Cembrene A from *Allokutzneria albata*. *Angew. Chem. Int. Ed.* *57*, 3238-3241.
- (46) Rabe, P., Rinkel, J., Nubbemeyer, B., Köllner, T. G., Chen, F. and Dickschat, J. S. (2016) Terpene Cyclases from Social Amoebae. *Angew. Chem. Int. Ed.* *55*, 15420-15423.
- (47) Rabe, P., Rinkel, J., Klapschinski, T. A., Barra, L. and Dickschat, J. S. (2016) A method for investigating the stereochemical course of terpene cyclisations. *Org. Biomol. Chem.* *14*, 158-164.
- (48) Rinkel, J. and Dickschat, J. S. (2019) Addressing the Chemistry of Germacrene A by Isotope Labeling Experiments. *Org. Lett.* *21*, 2426-2429.
- (49) Li, Z., Bally, T., Houk, K. N. and Borden, W. T. (2016) Variations in Rotational Barriers of Allyl and Benzyl Cations, Anions, and Radicals. *J. Org. Chem.* *81*, 9576-9584.

